Magnetoluminescence of GaAs in the quasiclassical limit

S. I. Gubarev,* T. Ruf, M. Cardona, and K. Ploog†
Max-Planck-Institut für Festkörperforschung, Heisenbergstrasse 1, D-7000 Stuttgart 80, Germany
(Received 28 January 1993)

We have observed very sharp lines in magnetoluminescence spectra of a GaAs-$Al_xGa_{1-x}As$ single heterostructure under resonant excitation of 10–70 meV above the GaAs direct energy gap. More than 14 lines were observed in both σ^+ and σ^- polarizations, at magnetic fields as low as 0.6 T. The spectral positions of these lines and their dependence on the magnetic field allow us to attribute the strongest lines to optical transitions between electron and light-hole Landau levels with indices from $n = 2$ to 15. The nonparabolicity of the bands and effects of the resonant electron-phonon interaction were directly observed in the luminescence spectra. The energies of optical transitions obtained for large Landau indices at low magnetic fields allow an accurate determination of band parameters in the classical limit. The effective mass and g factors of the light holes are found to be $m^*_{lh} = (0.078 \pm 0.002)m_0$ and $g^*_{lh} = 30.7 \pm 0.7$ for a magnetic field along the [001] direction.

I. INTRODUCTION

An external magnetic field applied to a semiconductor strongly influences the energy spectrum of free carriers in the conduction and valence bands, producing a set of Landau subbands with a quasi-one-dimensional dispersion law $E(k_z)$ in the direction along the magnetic field, separated by the cyclotron energies $\hbar\omega_c^{e,h}$. Since the optical transitions occur between appropriate Landau levels of conduction and valence bands, magneto-optical measurements provide important information about the effective masses of carriers and allow a set of band parameters to be obtained. Magneto-optical studies over the past 30 years have produced some of the most accurate values of the band parameters of elemental and $A_{III}B_V$ semiconductors.

The valence-band parameters of GaAs have been studied by different methods, such as magnetoabsorption,[1,2] magnetoreflectivity,[3] cyclotron-resonance absorption,[4] and recently by resonant magneto-Raman scattering.[5] In spite of numerous magneto-optical studies carried out on GaAs, the parameters obtained differ considerably even when measured by similar methods. (See, for example, the discussion in Ref. 6.)

Progress in GaAs molecular-beam-epitaxy-growth technology over the past decade has enabled high-quality GaAs crystals to be grown. Samples now available exhibit very sharp (full width at half maximum $\simeq 0.5$ meV) resonances in a magnetic field, which allows one to study the fine structure of interband magneto-optical transitions due to band admixing, as well as to study in detail the effects of the Coulomb and electron-phonon interaction on the energy spectrum of carriers in a magnetic field.

Recently, a new type of magneto-optical resonance in the spectra of hot photoluminescence resonantly excited at energies a few meV above interband transitions has been observed for a GaAs-$Al_{1-x}Ga_xAs$ heterostructure.[7] In this paper we present the results of a systematic study of this type of resonance. The sharpness of peaks observed allows us to determine with very good accuracy the energies of transitions between Landau subbands for different values of the magnetic field. More than 14 lines have been observed in both σ^+ and σ^- polarizations with widths as narrow as 0.5 meV. Deviation from linearity vs H due to band nonparabolicity and resonant electron-phonon interaction has also been noticed. The light-hole effective mass and g factor as well as nonparabolicity terms have been obtained from the data analysis.

The paper is organized as follows: In Sec. II we discuss the experimental method and the samples on which measurements were performed. In Sec. III the experimental results are presented. Section IV contains the analysis of experimental data. In Sec. V we summarize our results and make suggestions for future investigations. The paper includes Appendixes in which details of the calculations are presented.

II. EXPERIMENT

In the present study we used two types of GaAs samples, both grown on undoped [001] oriented substrates. Sample 1 was a 20-μm-thick epitaxial layer grown by liquid-phase epitaxy with an electron mobility of the order of $\mu \simeq 10^5$ cm^2/V s and electron concentration $N_d - N_a = 7 \times 10^{12}$ cm^{-3} at 77 K. The same sample was used in our previous experiments.[5] Sample 2 was a single heterojunction (SH) grown by molecular-beam epitaxy. Two micrometers of GaAs were covered with 1000-Å $Ga_{1-x}Al_xAs$ ($x = 0.33$) selectively doped with Si at 360 Å from the interface, so that a two-dimensional (2D) channel with a surface concentration of about $n_s = 2.2 \times 10^{11}$ cm^{-2} existed in the interface region. The high quality of the interface was confirmed by the large mobility of the 2D electrons ($\sim 10^6$ cm^2/V s) measured in this structure at liquid-helium temperature. We believe that the existence of such a high-quality in-

terface is essential for magnetoluminescence studies since luminescence properties of semiconductors are usually very sensitive to the surface quality. Resonant excitation above the fundamental absorption edge creates carriers close to the sample surface. A large density of surface states causes fast nonradiative recombination of the photocreated carriers, which decreases the lifetime of electrons in the crystal and leads to broadening of the electron states. In our case, the high quality of the interface seems to suppress surface recombination, with the corresponding narrowing of the luminescence lines and enhancement of their intensities.

The data obtained on sample 1 (bulk GaAs) and sample 2 (wide buffer SH) are rather similar. No differences in energy positions and relative intensities of the peaks were observed within the experimental accuracy; however, the absolute intensities of magnetoluminescence peaks were found to be one order of magnitude stronger in sample 2, which also exhibited features with an approximately 30% narrower linewidth, due to the suppression of surface recombination. For this reason most of the data presented below were obtained with sample 2. One should expect in the magnetoluminescence spectra of sample 2 also some features related to Landau levels arising from 2D electron states confined in the region of the interface. The comparison of resonance profiles measured on both samples shows that peaks from bulk Landau levels dominate. We attribute this to the large width of the GaAs layer in sample 2. The bulklike states are much less perturbed by the interface than the rather localized 2D states which therefore have shorter lifetimes and are suppressed under resonant excitation. For these reasons we shall refer to both samples studied as GaAs samples in the following.

The experiments were performed in magnetic fields of $H \leq 14$ T with a sample temperature of about 5 K. We used an Oxford Instruments 14/16T superconducting magnet with a 52 mm bore diameter and field uniformity better than 0.1% in the spherical volume of 1 cm^3. Magnetoluminescence spectra in the range of 1520–1600 meV were studied in backscattering geometry with the magnetic field applied perpendicular to the layer surface. To realize resonant excitation conditions we used a tunable Ti-sapphire laser pumped with a cw Ar^+-ion laser. The laser excitation power was restricted to less than 3 mW, with a spot size of 0.5 mm^2 in order to decrease the effects of exciton-exciton interaction and prevent sample heating. Most of the data were taken in Faraday geometry in the $z(\sigma^+\sigma^+)\bar{z}$ and $z(\sigma^-\sigma^-)\bar{z}$ polarizations, i.e., the excitation and detection were performed in the same circular polarization. For most of the measurements a double monochromator was set as spectral band pass at the energy of 2–5 meV below the laser energy. The luminescence intensity was then measured as a function of the magnetic field. A small hysteresis of about 20 mT was found between scans with increasing and decreasing magnetic fields at a rate of 0.6 T/min and this difference was taken into account in the following data analysis. To obtain the exciton ground-state energy, luminescence spectra excited by the green lines of the Ar^+-ion laser were also studied in magnetic fields up to 14 T.

III. EXPERIMENTAL RESULTS

Figure 1 gives the luminescence spectrum of sample 2 at zero magnetic field under excitation by the green lines of an Ar^+ laser. The bulk-exciton luminescence line at the energy $E_{1S} = 1515.1$ meV dominates the spectrum. This assignment to the bulk exciton is in accord with the literature value of E_{1S} =1515.01 meV (Ref. 8) and also agrees with the results of our magnetoreflectivity study. On the high-energy side of the $1S$-exciton line an additional feature at $E_{n=2} = 1518.2$ meV was observed, which corresponds to the exciton excited state ($n = 2$). Some traces of bound-exciton complexes appear on the low-energy side of the free-exciton line. The good resolution of the $n = 1$ and $n = 2$ exciton lines and the low intensity of the bound-exciton lines indicate the low concentration of structural defects and residual impurities in our samples. The spectral positions of all luminescence lines observed at $H = 0$ are consistent with those of the bulk exciton recombination given in the literature.[9]

Figure 2 shows typical luminescence spectra taken at magnetic fields between 6 and 6.8 T in small steps $\Delta H = 0.2\ T$ under resonance excitation at $E_L = 1583$ meV. At energies of a few meV below the laser energy a rather narrow line is observed, with both its energy position and intensity being strongly dependent on the magnetic field. With increasing field, the line shifts rapidly towards higher energies and its intensity increases by about two orders of magnitude. The spectral position of such a luminescence line has been found to depend only on the magnetic field, while its intensity is mainly controlled by its energy separation from the exciting laser energy $\Delta = E_L - E_S$. With increasing Δ, the signal intensity drops rapidly, and for $\Delta \geq 7$ meV it is too low for reliable measurements. When we set the monochromator at an energy a few meV below the laser (in what follows, most data were taken at $\Delta = E_L - E_S = 2$ meV) and measure the luminescence intensity $I(H)$ as a function of magnetic field, a series of resonances is observed in the $I(H)$ profile. Figure 3 shows such profiles taken in the $z(\sigma^+\sigma^+)\bar{z}$

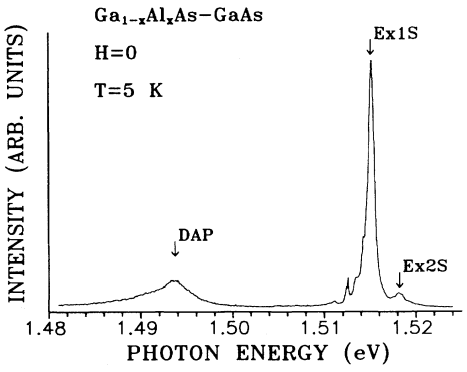

FIG. 1. The spectrum of bulk luminescence of GaAs-$Ga_{1-x}Al_xAs$ samples near the fundamental gap of GaAs taken at $H = 0$, $T = 5$ K. Arrows show positions of the $n = 1$ and $n = 2$ exciton terms and donor-acceptor pair recombination (DAP).

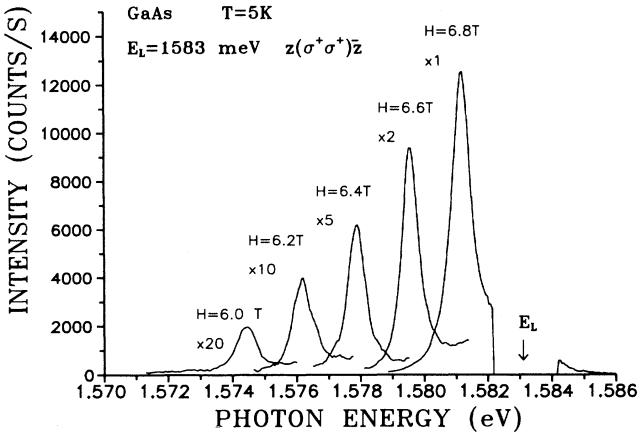

FIG. 2. Luminescence spectra of GaAs in $z(\sigma^+\sigma^+)z$ configuration for different values of magnetic field H for exciting photons with $E_L = 1583$ meV.

and $z(\sigma^-\sigma^-)\bar{z}$ configurations at $E_S = 1571$ meV and $E_L = 1573$ meV. Sharp and narrow resonances start at very low magnetic fields $H \leq 1$ T, with their intensities increasing up to 10^4 counts/s for $H > 5$ T. These peaks correspond to successive interband optical transitions between Landau levels and occur whenever their energy matches with that of the spectrometer.

The large difference in peak positions for the two circular polarized configurations (large effective g factor) indicates that light-hole levels are involved in the optical transitions observed.[5] To distinguish between resonant luminescence and Raman-scattering contributions we also performed measurements for different excitation energies with the luminescence being detected at a fixed energy (see Fig. 4). We found the positions of the main peaks in magnetoluminescence spectra $I(H)$ to be independent of the laser energy and determined only by the detection energy. The variation of the laser energy only affects the intensity of the peaks observed which decreases strongly with increasing energy difference $\Delta = E_L - E_S$ between excitation and detection energies. On the high-field side of the magnetoluminescence lines one can also see small peaks, which result from resonance in the excitation channel; these peaks occur when the laser energy coincides with the energy of interband transitions with a corresponding increase in the luminescence background.

This method has allowed us to obtain a wealth of experimental information about the energies of magneto-optical transitions in the region of 1525 meV $\leq E_s \leq$ 1595 meV. Even with low excitation power, $P \leq 3$ mW, the typical intensities of the magnetoluminescence peaks are of the order of 10^4 counts/s. At energies lower than 1525 meV a strong background due to the exciton ground-state luminescence disturbs the magnetoluminescence profiles. At energies around $E_s = 1590$ meV we observed a threshold where the intensity of luminescence peaks decreases drastically (see Fig. 5). This behavior is more pronounced in the $z(\sigma^+\sigma^+)\bar{z}$ geometry,

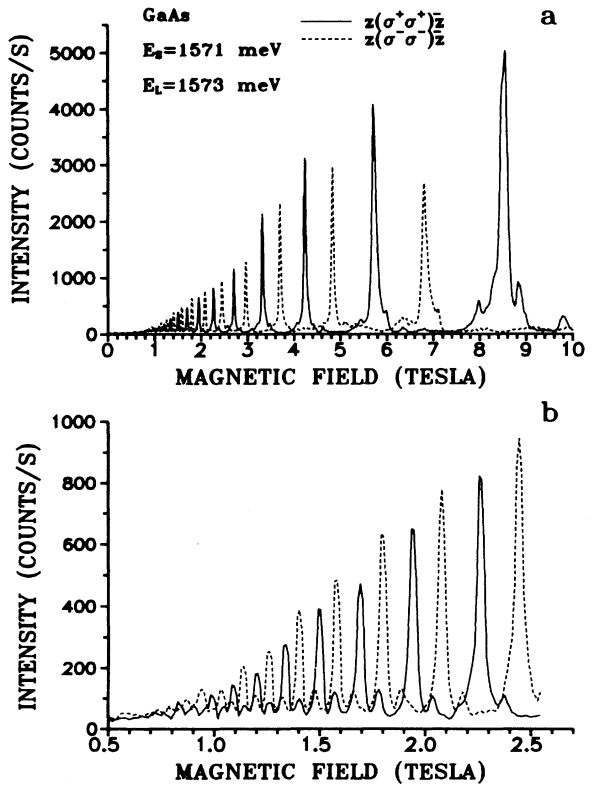

FIG. 3. Magnetoluminescence profiles $I(H)$ measured in $z(\sigma^-\sigma^-)\bar{z}$ (dashed line) and $z(\sigma^+\sigma^+)\bar{z}$ (solid line) configurations. E_S =1571 meV, E_L = 1573 meV, Δ = 2 meV. The lower part (b) shows the low magnetic-field domain.

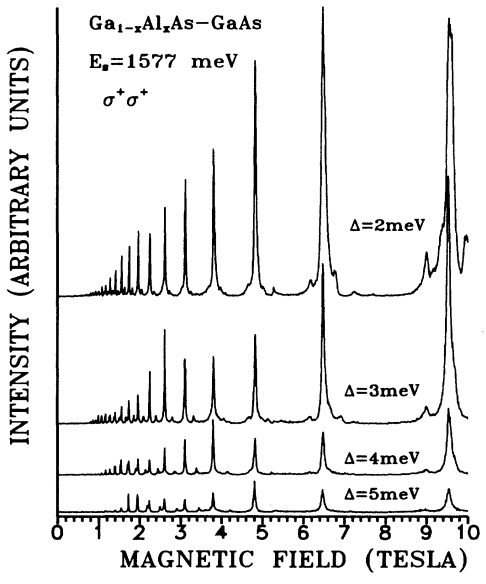

FIG. 4. Magnetoluminescence profiles $I(H)$ measured at the same energy E_s = 1577 meV, but with different laser excitation energies E_L. The energy separation $\Delta = E_L - E_S$ is given next to each plot.

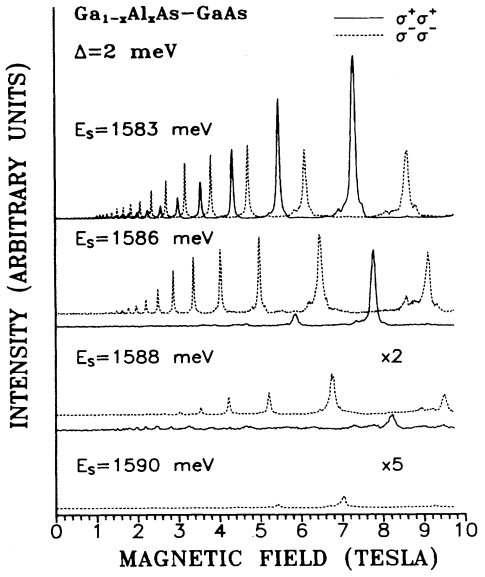

FIG. 5. Magnetoluminescence profiles $I(H)$ taken in $z(\sigma^+\sigma^+)\bar{z}$ geometry (solid lines, $b_n^+ \rightarrow \beta_n$ transitions) and in $z(\sigma^-\sigma^-)\bar{z}$ geometry (dotted lines, $a_{n+2}^+ \rightarrow \alpha_n$ transitions) for different detection energies E_s. The plots demonstrate the washout of magnetoluminescence resonances, when the optical transition energy becomes close to the magnetopolaron threshold.

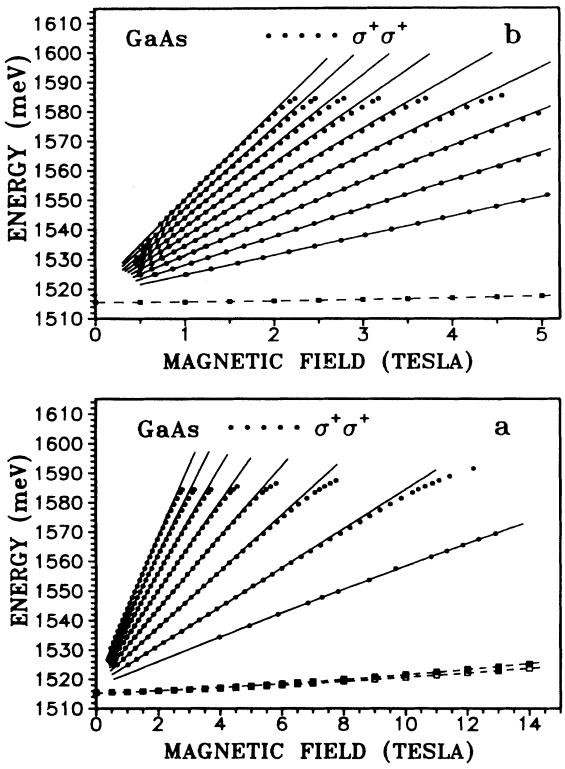

FIG. 6. Fan plots of magnetoluminescence resonances in $z(\sigma^+\sigma^+)\bar{z}$ (•) ($b_n^+ \rightarrow \beta_n$, optical transitions) configuration. The lines are fits with an expression quadratic in H of the points in the low-energy range 1530 meV $\leq E_s \leq$ 1570 meV. The positions of exciton ground states measured from luminescence spectra are shown by squares. The upper part (b) shows fan lines at low magnetic fields.

where an increase of the energy by only 3 meV practically leads to the disappearance of the magnetoluminescence signal. When E_S increases, the larger index peaks disappear before those with the smaller indices. In the $z(\sigma^+\sigma^+)\bar{z}$ configuration the threshold occurs at energies of about $E_s \approx 1585$ meV and in $z(\sigma^-\sigma^-)\bar{z}$ configuration at $E_s \approx 1590$ meV. It will be shown later that these values correspond to carrier energies about 1 LO phonon above the bottom of the conduction band. Fast energy relaxation due to emission of optical phonons becomes possible in this case, producing a strong decrease in "hot-electron" populations and a broadening of the corresponding levels. The intensity of the magnetoluminescence peaks $I(H)$ drops then by more than two orders of magnitude, which makes the study of resonant luminescence problematic. In what follows, we shall focus our attention on resonance behavior in the energy region $E_S, E_L < 1590$ meV, where intense and narrow peaks are observed.

As we have already mentioned, the small width of the resonance peaks (for numbers $n \geq 7$ it is less than 0.02 T) allows an accurate measurement of the transition energies between Landau subbands with large indices n. Figures 6 and 7 give the positions of dominant peaks in the magnetoluminescence spectra $I(H)$ measured at different energies in $z(\sigma^+\sigma^+)\bar{z}$ and $z(\sigma^-\sigma^-)\bar{z}$ configurations; transition energies form well defined sets as a function of magnetic field H. The upper parts of these figures display the behavior of these "fan plots" in the region of low magnetic fields. The lines in these figures represent quadratic fits with for energies below 1570 meV (for details of the fitting procedure see the next section). The same figures also give the exciton ground-state energies measured from luminescence with Ar^+-ion laser excitation. One can see that when $H \rightarrow 0$ the sets of peaks in both the $z(\sigma^+\sigma^+)\bar{z}$ and $z(\sigma^-\sigma^-)\bar{z}$ polarizations converge to the same energy $E_0 \approx 1518$ meV, which is close to the direct gap of GaAs. Fan lines $E(H)$ in both circular polarization configurations exhibit pronounced deviations from parabolic behavior at energies around 1590 meV, where resonant electron-LO-phonon interaction (magnetophonon resonance) becomes possible.[10,11] These deviations will be discussed in more detail in Sec. IV.

IV. DISCUSSION

A. Theory

The fundamental gap of GaAs occurs at the Brillouin-zone center (Γ point), where the states transform according to the point group symmetry T_d. Including spin-orbit coupling, the s-like conduction band transforms as Γ_6^c ($J = \frac{1}{2}$), and the triply degenerate p-like valence band splits into bands transforming as Γ_8^v ($J = \frac{3}{2}$) or

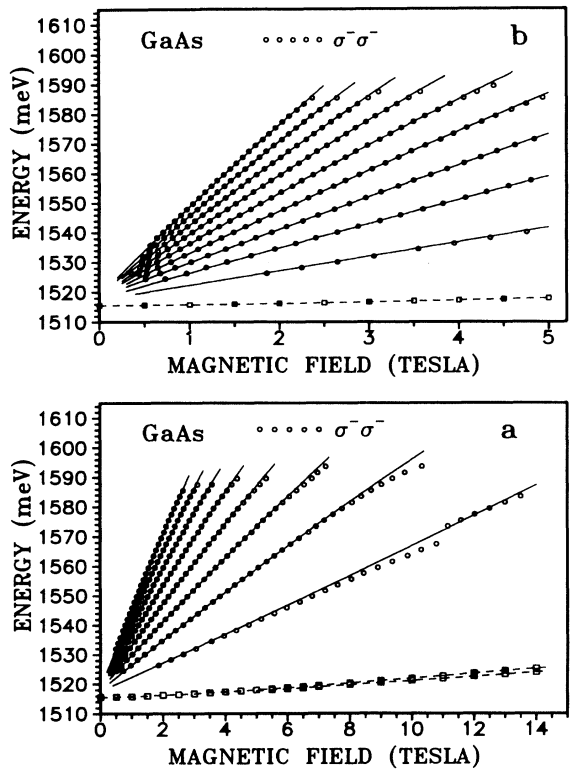

FIG. 7. The same as Fig. 6 but for $z(\sigma^-\sigma^-)\bar{z}$ geometry ($a^+_{n+2} \to \alpha_n$, optical transitions).

Γ^v_7 ($J = \frac{1}{2}$) with the energy splitting Δ_0. The wave functions of the electron states at Γ ($k = 0$) can be written in the Kohn-Luttinger representation[12] as

$$\begin{aligned} u^c_1 &= S\alpha, \\ u^c_2 &= S\beta, \\ (m_j = 3/2)\quad u^v_1 &= 2^{-1/2}(X + iY)\alpha, \\ (m_j = 1/2)\quad u^v_2 &= i6^{-1/2}[(X + iY)\beta - 2Z\alpha], \\ (m_j = -1/2)\quad u^v_3 &= 6^{-1/2}[(X - iY)\alpha + 2Z\beta], \\ (m_j = -3/2)\quad u^v_4 &= i2^{-1/2}(X - iY)\beta, \end{aligned} \tag{1}$$

where S, X, Y, and Z transform under T_d like atomic s, p_x, p_y, and p_z functions, and α and β indicate states with spin up and down, respectively.

In a magnetic field the bands are quantized into Landau subbands. There are two sets of Landau subbands in the conduction band corresponding to different spins $\sigma = \alpha, \beta$ with energies

$$\epsilon^c_\sigma = \epsilon_g + \hbar\omega^e_c\left(n + \frac{1}{2}\right) + \frac{\hbar^2 k_z^2}{2m^*_e} + \mu_B g^*_e \sigma H \tag{2}$$

and wave functions

$$\Psi^c_n = u^c_{k,\sigma}(r)\Phi_n(r), \quad \sigma = \alpha, \beta, \tag{3}$$

$$\Phi_n(r) = \frac{1}{L}\exp\left[i\left(k_z z + k_x x\right)\right]\phi_n\left(\frac{y - y_0}{\lambda_H}\right),$$

where $\omega^e_c = eH/m^*_e c$ is the cyclotron frequency, $\lambda_H = (c\hbar/eH)^{1/2}$ the magnetic length, n the Landau level index, and $\phi_n(r)$ a harmonic-oscillator wave function.

The degenerate valence band Γ^v_8 forms four series (ladders) of nonequally spaced levels $|a^+_n\rangle$ and $|b^+_n\rangle$, which correspond for large n to light holes, and $|a^-_n\rangle$ and $|b^-_n\rangle$, which correspond to heavy holes. Because of degeneracy of the Γ^v_8 band at $k = 0$ the external magnetic field mixes the valence states even to zeroth order in H. For nearly spherical bands and $k_z = 0$, the problem was solved by Luttinger,[13] who also formulated a perturbation approach to the anisotropic problem. In this approach, the problem reduces to the diagonalization of two 2×2 matrices and allows an analytical solution. The valence states decouple into two sets with energies (in magnetic units $s = \hbar eH/m_0 c$)

$$\epsilon^\pm_a(n) = \gamma_1 n - L_{1a} \pm \left[\left(\gamma' n - L_{2a}\right)^2 + 3\gamma''^2 n(n-1)\right]^{1/2} \tag{4}$$

for set a and

$$\epsilon^\pm_b(n) = \gamma_1 n - L_{1b} \pm \left[\left(\gamma' n + L_{2b}\right)^2 + 3\gamma''^2 n(n-1)\right]^{1/2} \tag{5}$$

for set b, with

$$\begin{aligned} L_{1a} &= \frac{1}{2}\gamma_1 + \gamma' - \frac{1}{2}\kappa, & L_{2a} &= \gamma_1 - \kappa + \frac{1}{2}\gamma', \\ L_{1b} &= \frac{1}{2}\gamma_1 - \gamma' + \frac{1}{2}\kappa, & L_{2b} &= \gamma_1 - \kappa - \frac{1}{2}\gamma', \end{aligned} \tag{6}$$

where γ_1, γ', γ'', κ are the Luttinger parameters describing the valence band of a cubic semiconductor in a magnetic field. The parameters γ' and γ'' depend on the direction of the magnetic field with respect to the crystallographic axes. In the case $H \parallel [001]$ they are connected with the Luttinger parameters γ_2 and γ_3 through the relations $\gamma' = \gamma_2$ and $\gamma'' = (\gamma_2 + \gamma_3)/2$. For the definition of γ_1, γ_2, and γ_3 see Ref. 13 and Appendix A.

The wave functions designated here by the index n are combinations of n and $n-2$ harmonic-oscillator states:

$$\begin{aligned} \Psi^{a\pm}_n &= |a^\pm_n\rangle = a^\pm_1 u^v_1(r)\Phi_{n-2}(r) + a^\pm_2 u^v_3(r)\Phi_n(r), \\ \Psi^{b\pm}_n &= |b^\pm_n\rangle = b^\pm_1 u^v_2(r)\Phi_{n-2}(r) + b^\pm_2 u^v_4(r)\Phi_n(r). \end{aligned} \tag{7}$$

The cyclotron frequencies $\omega_\pm$ for the light and heavy holes in the classical limit (large n) are the same for holes from the a and b sets and are given by

$$\omega_\pm \approx \frac{eH}{m_0 c}\left[\gamma_1 \pm \left(\gamma'^2 + 3\gamma''^2\right)^{1/2}\right]. \tag{8}$$

The Luttinger solution is linear in the magnetic field, with the cyclotron masses of holes for large n depending only on the direction of the field with respect to the crystal axes. This is due to the fact that in the Luttinger scheme only states from the Γ^v_8 multiplet are coupled by the magnetic field, while explicit coupling with

other bands is neglected. This coupling was taken into account by Pidgeon and Brown (PB),[14] who treated the Γ_7^v, Γ_8^v and Γ_6^c states in an 8×8 $\mathbf{k} \cdot \mathbf{p}$ scheme. This approach was developed further in the papers of Suzuki and Hensel,[15] Aggarwal,[16] Weiler, Aggarwal, and Lax[17] and Trebin, Rössler, and Ranvaud.[18] The authors of Ref. 18 analyzed the terms in the Hamiltonian in accordance with the different symmetry classes and introduced terms which occur, because of inversion asymmetry, in zinc-blende semiconductors. The coupling with conduction and spin-orbit-split bands leads to an additional mixing of wave functions as compared with that described by the Luttinger solution. As a result, a deviation from a linear behavior with H occurs for electron and hole energies (nonparabolicity) and some otherwise dipole forbidden transitions become allowed. Effects of nonparabolicity on the effective masses of conduction and valence bands will be discussed in more detail in the next section and in Appendix B.

Selection rules for the interband magneto-optical transitions follow from the mixed cyclotron orbital character of the valence-band wave functions. In contrast to simple bands, where transitions are allowed only between levels with the same Landau indices $n_e = n_h$, $\Delta n = 0$, the degenerate valence bands of GaAs allow, even in the spherical approximation, optical transitions with $\Delta n = 0, -2$. The optical transitions allowed in the σ^+, σ^-, and π ($\mathbf{e}_z \parallel \mathbf{H}$) polarizations can be summarized as follows:[19]

$$\begin{aligned} &|a_n^{\pm}\rangle \rightarrow |\alpha_n\rangle, \quad |b_n^{\pm}\rangle \rightarrow |\beta_n\rangle; \quad (\sigma^+) \\ &|a_n^{\pm}\rangle \rightarrow |\alpha_{n-2}\rangle, \quad |b_n^{\pm}\rangle \rightarrow |\beta_{n-2}\rangle; \quad (\sigma^-) \\ &|a_n^{\pm}\rangle \rightarrow |\beta_n\rangle, \quad |b_n^{\pm}\rangle \rightarrow |\beta_{n-2}\rangle, \quad (\pi) \end{aligned} \tag{9}$$

respectively. In Faraday configuration only transitions in circular polarization are possible with the selection rules $\Delta n = 0$ in σ^+ and $\Delta n = -2$ in σ^- polarizations.

There is some confusion in the literature concerning the indexing of the valence subbands. Two schemes are found. One, proposed by Luttinger, is used in Refs. 19 and 1. In this scheme, which we also use in our paper, the valence-band wave functions have the form (7) and are a combination of two oscillator wave functions, with an index referring to the largest oscillator quantum number n. The second scheme has its origin in the PB approach and was used in Refs. 16 and 20. The PB approach is based on the diagonalization of an 8×8 $\mathbf{k} \cdot \mathbf{p}$ Hamiltonian with the Γ_6^c, Γ_8^v, and Γ_7^v wave functions as basis. The main coupling occurs between levels n in the conduction band, and levels $(n-1)$ and $(n+1)$ of the valence band. The eigenvectors in this scheme are a combination of conduction- and valence-band wave functions where n refers to the conduction band. This leads to the selection rules $\Delta n = n_c - n_v = \pm 1$. The apparent difference in the selection rules is fictious and is connected with a different scheme of indexing Landau levels in the valence band arising from the different perturbation theory schemes used.

B. Data analysis

The behavior of the discussed magnetoluminescence peak energies as a function of the magnetic field directly indicates that these peaks arise from interband magneto-optical transitions between different Landau levels in conduction and valence bands. The energy of an optical interband transition equals the sum of gap energy ε_g, and the magnetic energies of the electron and hole participating in the recombination process, reduced by the Coulomb interaction between electron and hole,

$$\varepsilon_{mn}(H) = \varepsilon_g + \varepsilon_{\lambda m}^h(H) + \varepsilon_{n,\sigma}^e(H) - R_{mn}^{\lambda\sigma}(H), \tag{10}$$

where $\lambda = a^+, b^+, a^-, b^-$; $\sigma = \alpha, \beta$; magnetic energies ε^e, ε^h of carriers are energies of Landau levels with respect to the bottom of the conduction band and the top of the valence band, respectively, both being positive for conduction- and valence-band levels; and $R_{mn}^{\lambda\sigma}(H)$ is the energy of Coulomb correlations between electron and hole involved in the optical transition.

The selection rules discussed in the preceding paragraph allow transitions with $n = m$ in σ^+ polarization and $n = m - 2$ in σ^- polarization. Using the results of magnetoabsorption studies,[1,2,21] the main peaks in magnetoluminescence profiles have been attributed to the transitions $b_n^+ \rightarrow \beta_n$ in the σ^+ polarization and $a_{n+2}^+ \rightarrow \alpha_n$ in the σ^- polarization. Between the main peaks others with a much smaller intensity were also seen, which probably correspond to optical transitions $b_{n+2}^+ \rightarrow \beta_n$ and $a_n^+ \rightarrow \alpha_n$. The position of these peaks was measured with a much lower accuracy because their shape is strongly disturbed by a background arising from the main peaks. We will not discuss therefore their behavior, but rather focus our attention on the main peaks.

When analyzing the optical transition energies, corrections to the electron-hole Coulomb interaction have to be made. A general theory describing exciton states in the intermediate range of magnetic fields is not available. We estimated the exciton corrections using a quasiclassical approach which was recently proposed to describe Coulomb correlations for electron states with large Landau indices n (see Appendix C for details).

We are interested in the slope of the fan plots $E_{mn}(H)$ as a function of magnetic field H for different levels involved in the optical transitions. We shall first use an empirical description of the optical transitions and then connect it with the band parameters of GaAs. We fit the energies of optical transitions with the expansion

$$\varepsilon_{mn} = \epsilon_0 + \epsilon_1 H - \epsilon_2 H^2. \tag{11}$$

This description is based on Aggarwal's analysis,[16] who considered the energies of magneto-optical transitions within the framework of the 8×8 $\mathbf{k} \cdot \mathbf{p}$ model, and derived expressions for the energies of the electron and light holes by expanding the secular equation in powers of the magnetic energies $s = \hbar eH/m_0 c$. Except for corrections due to Coulomb interaction, ϵ_0 in expression (11) is the gap energy at $H = 0$, ϵ_1 is related to the reduced optical mass, and ϵ_2 represents the sum of nonparabolic contributions arising from valence and conduction bands.

The energies of magneto-optical transitions were fitted by the least-squares method in the 1530–1570 meV range. To reduce the resonant polaron effects, only data below 1570 meV were taken into account. Parameters obtained from the fit were found to be insensitive to the choice of the high-energy limit up to $E \approx 1575$ meV, where the influence of magnetophonon resonance on the energies of electron states becomes appreciable. The results of the fitting procedure performed for the optical transitions in σ^+ and σ^- polarizations are displayed in Figs. 6 and 7 by solid lines. From this fitting we obtained the coefficients ϵ_0, ϵ_1, and ϵ_2 for the transitions $b_n^+ \rightarrow \beta_n$ $(2 \leq n \leq 10)$ and for transitions $a_{n+2}^+ \rightarrow \alpha_n$ $(1 \leq n \leq 9)$.

All the fan lines converge to the same energy ϵ_0 within 1 meV for $H \rightarrow 0$, (ϵ_0 increases monotonically from 1517.8 meV for transitions with low numbers $n = 2$ to 1518.5 meV for transitions with $n \geq 5$).

The linear coefficient $\epsilon_1 = \epsilon_1^c + \epsilon_1^{\rm lh}$ in (11) describes the slope of fan lines for low magnetic fields ($H \rightarrow 0$) and is thus connected with the electron and light-hole masses at $k = 0$. It can be expressed in terms of the electron mass and Luttinger parameters, neglecting electron spin, as follows:

$$\epsilon_1^{mn} = \frac{1}{m_e^*}\left(n + \frac{1}{2}\right) + \epsilon_\lambda(m) \ , \tag{12}$$

where $m = n$ for the σ^+ polarization and $m = n + 2$ for the σ^- polarization and the $\epsilon_\lambda(m)$ $(\lambda = a^+, b^+)$ are given by Luttinger expressions (4) and (5).

The slopes $\epsilon_1(n)$ of the optical transitions $b_n^+ \rightarrow \beta_n$ and $a_{n+2}^+ \rightarrow \alpha_n$ are displayed in Fig. 8 as functions of the index n. Their behavior is linear with n and, for the optical transitions with indices $n \geq 5$, it can be described by the following expressions: for $b_n \rightarrow \beta_n$ transitions (σ^+ polarization)

$$\epsilon_1(b_n \rightarrow \beta_n) = (3.242\ n + 0.78)\ \text{meV/T} \tag{13}$$

and for $a_{n+2} \rightarrow \alpha_n$ transitions (σ^- polarization)

$$\epsilon_1(a_{n+2} \rightarrow \alpha_n) = (3.246\ n + 2.54)\ \text{meV/T} \ . \tag{14}$$

The change of the slope $\epsilon_1(n) - \epsilon_1(n-1)$ in the limit of large n is connected with the reduced cyclotron masses of the electron and light hole

$$\epsilon_1(n) - \epsilon_1(n-1) = \mu^{-1} = \frac{1}{m_e} + \frac{1}{m_{\rm lh}} = \frac{1}{m_e} + \gamma_1 + \left(\gamma'^2 + 3\gamma''^2\right)^{1/2} . \tag{15}$$

Equations (13) and (14) give us the value of the reduced mass $\mu^{-1} = m_e^{-1} + m_{\rm lh}^{-1} = 28.02 m_0^{-1}$. Using the electron effective-mass value $m_e^* = 0.0660 m_0$, obtained recently from cyclotron resonance with corrections for nonparabolicity,[22] we found for the light-hole mass $m_{\rm lh}[H \parallel (001)] = (0.078 \pm 0.002) m_0$, which is approximately 10% smaller than the previously reported values.[9] We believe that the difference in band parameters in comparison with other magneto-optical studies is mainly due to our more accurate treatment of nonparabolicity effects. The light-hole masses have been calculated recently for GaAs using the five-level $\mathbf{k} \cdot \mathbf{p}$ model.[23] These calculations give the cyclotron mass of the light hole for $H \parallel (001)$ as $m_{\rm lh} = 0.0755 m_0$, which is in good agreement with our result. The light-hole mass determined in the present work is also more consistent with the parameters generally used in $\mathbf{k} \cdot \mathbf{p}$ calculations than other data (see Appendix A). We have found that Coulomb corrections to the interband transition energies decrease rapidly with increasing Landau index n and with decreasing magnetic field. For large numbers $n \geq 4$ and magnetic fields in the range of 1 T$< H <$ 5 T these corrections give a contribution to the slope $\partial E / \partial H$ of less than 5%. We would like to note that neglecting exciton corrections during the fitting procedure gives an even lower value $m_{\rm lh} = 0.075 m_0$ for the light-hole mass.

From the difference between the lines in Fig. 8 the optical effective g factor[24] of the light hole can be determined to be $g_{\rm lh} = 2(\gamma_1 + 2\tilde{\gamma} + 2\kappa) = 30.7 + g_e^*$. This gives the Luttinger parameter $\kappa = (g_{\rm lh} - 2/m_{\rm lh})/4 = 1.25 \pm 0.2$, which is consistent with the published value [$\kappa = 1.2 \pm 0.2$ (Ref. 9)].

It can be seen in Figs. 6 and 7 that pronounced deviations from the fitted parabolic behavior occur at a transition-energy threshold of around 1590 meV. This bending of the fan lines is ascribed to resonant electron-phonon interaction between the higher Landau levels n and the $n = 0$ state. Whenever the energy difference between such electron levels equals the LO phonon energy, an anticrossing occurs in the electronic structure with the n state becoming clamped to the $n = 0$ ground-state level for higher magnetic fields. Due to the small value of

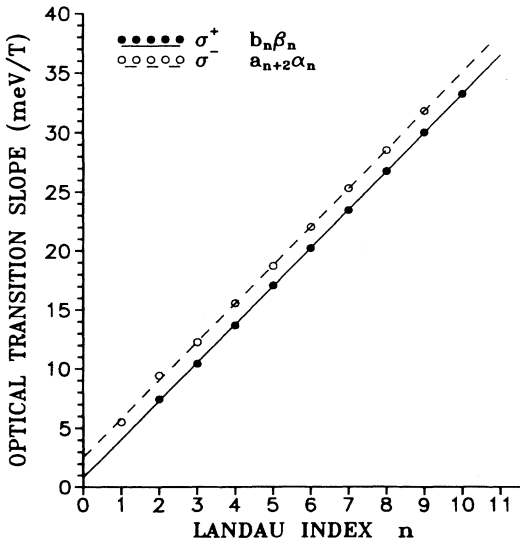

FIG. 8. Slopes of the optical transitions $\partial\varepsilon/\partial H$ at $H \rightarrow 0$ as function of the Landau index n. The experimental data are represented by ○ and • for $b_n^+ \rightarrow \beta_n$ and $a_{n+2}^+ \rightarrow \alpha_n$ optical transitions, respectively. Lines are linear fits of the points with $n \geq 4$.

the Fröhlich coupling constant α_F in GaAs [$\alpha_F = 0.065$ (Ref. 9)], these anticrossings are usually hard to observe in interband magneto-optical experiments. Our high-quality sample used allowed us to resolve resonant magneto-polaron effects up to $n = 9$. Deviations of the fan-plots from parabolic behavior in the vicinity of magneto-phonon resonances are in good agreement with a theory[25] proposed recently for description of resonant polaron corrections to the lower branch of Landau subbands with arbitrary index n. We found that resonant polaron corrections do not influence the slope of optical transitions at $H \to 0$, while they give a noticeable contribution to the nonparabolic term ε_2 even at energies lower than 1570 meV. Their contribution is about 20% of the total nonparabolicity and was subtracted from experimental fan lines before fitting them with Eq. (11).

The corrections to the optical transition energies quadratic in H can be written as (see Appendix B)

$$\epsilon_2 = \frac{(\varepsilon_1^c)^2}{\varepsilon_c^*} + \frac{(\varepsilon_1^{\rm lh})^2}{\varepsilon_{\rm lh}^*} , \tag{16}$$

where ε_1^c ($\varepsilon_1^{\rm lh}$) is the contribution linear in H to the electron (hole) energy and ε_c^* and $\varepsilon_{\rm lh}^*$ are effective parameters with dimensions of energy.

Figure 9 displays the experimental values of $\epsilon_2^{1/2}$ and those calculated with Eq. (16) for the $a_{n+2}^+\alpha_n$ and $b_n^+\beta_n$ transitions as function of the transition index n. The electron mass $m_e = 0.0660 m_0$ was used to calculate the conduction-band energy ε_1^c. The hole energy $\varepsilon_1^{\rm lh}$ was obtained from the experimentally measured value $\varepsilon_1 = \varepsilon_1^c + \varepsilon_1^{\rm lh}$ by subtracting the conduction-band contribution. The parameters $\varepsilon_c^* = 1.31$ eV and $\varepsilon_{\rm lh}^* = 0.47$ eV were calculated with $\mathbf{k}\cdot\mathbf{p}$ theory (see Appendix B). The theoretical values describe the observed band nonparabolicity reasonably well. It follows from the $\mathbf{k}\cdot\mathbf{p}$ theory (see Ref. 1 and Appendix) that the coefficients $\epsilon_2^c(n)$ and $\epsilon_2^{\rm lh}(n)$ which describe the nonparabolicity increase quadratically with the transition index n. This leads to an approximately linear increase of $\epsilon_n^{1/2}$ with n. Such a behavior is consistent with experimental observations. Expression (B7) also satisfactorily describes the larger nonparabolicity observed for the $a_{n+2}\alpha_n$ set of transitions with respect to the $b_n\beta_n$ set, arising from a larger hole contribution to the transition energy $\epsilon_{n+2}^a > \epsilon_n^b$. However, the nonparabolicity observed is systematically 15–20 % stronger than the calculated one. A somewhat better fit can be achieved with the parameters $\epsilon_c^* \approx 1$ eV and $\epsilon_{\rm lh}^* \approx 0.41$ eV. It is interesting to note that an empirical fit of the cyclotron resonance data also gives a value for ϵ_c^* lower than 1.31 eV ($\epsilon_c^* \approx 0.98$ eV from Ref. 23), which is consistent with our findings. We also mention that at energies 1.53 eV $< E_S <$1.57 eV, where most data were taken, the nonparabolic corrections to the electron and hole magnetic energies are much smaller than in typical magnetoabsorption experiments[1,21] where the energies up to 1.7 eV were used in determination of band parameters. The influence of these corrections on the transition energy is thus much lower in our case than in previous studies.

Another advantage of the present measurements as compared to previous magnetoabsorption studies of GaAs (Refs. 1, 2, and 21) is that the main information is obtained from optical transitions corresponding to large Landau indices $n \geq 5$ where quantum-defect corrections to the hole mass are small and the light-hole mass approaches its classical value. Under such conditions corrections due to Coulomb interaction are strongly reduced. This makes the uncertainty in the estimation of exciton corrections smaller than in previous studies.

The method presented here has the potential to yield similar high-precision results in other bulk and microstructured semiconductors. We have in fact observed similar magnetoluminescence resonances in InP and CdTe.

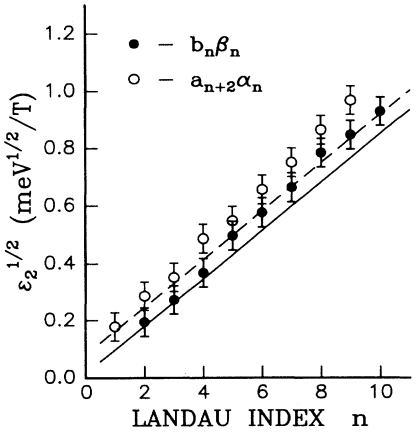

FIG. 9. Nonparabolic coefficients $\epsilon_2^{1/2}$ as a function of Landau index n for $b_n^+ \to \beta_n$ (•) and $a_{n+2}^+ \to \alpha_n$ (○) optical transitions. The lines display results of calculations with effective two level parameters $\varepsilon_c^* = 1.31$ eV and $\varepsilon_{\rm lh}^* = 0.47$ eV (see text for details).

V. CONCLUSIONS

The energies of interband magneto-optical transitions between different Landau subbands were investigated by studying the magnetoluminescence spectra of GaAs under resonance laser excitation. The luminescence efficiency was increased through the use of a GaAs-$Al_xGa_{1-x}As$ single heterojunction with a high-quality interface which results in suppression of surface recombination. The observed resonances of the luminescence intensity give very precise information on the energy spectrum of carriers in a magnetic field. The effects of electron and light-hole band nonparabolicity and resonant electron-phonon interaction have been directly seen in our measurements. As a result of the data analysis, the light-hole mass and g factor have been obtained as well as coefficients for the nonparabolicity of the light-hole band. The light-hole mass has been found to be $m_{\rm lh} = (0.078 \pm 0.002) m_0$, 10% smaller than previously measured values but in good agreement with recent calculations and consistent with parameters used in $\mathbf{k}\cdot\mathbf{p}$ calculations.

ACKNOWLEDGMENTS

We are very thankful to Professor E. Burstein for a critical reading of the manuscript. Useful discussions with Dr. V. Falko are gratefully acknowledged. Thanks are also due to H. Hirt, M. Siemers, and P. Wurster for expert technical help. S.I.G. would like to acknowledge the financial support from the Alexander von Humboldt Foundation.

APPENDIX A: COMPARISON WITH $\mathbf{k}\cdot\mathbf{p}$ BAND CALCULATIONS

It is interesting to compare the results of our measurements with band parameters used in $\mathbf{k}\cdot\mathbf{p}$ band calculations. The shape of the Γ_8^v valence band of GaAs around $\mathbf{k}=0$ is given by[26]

$$E(k)=Ak^2\pm\left[B^2k^4+C\left(k_x^2k_y^2+k_y^2k_z^2+k_z^2k_x^2\right)\right]^{1/2}, \tag{A1}$$

where

$$\begin{aligned} A&=\frac{1}{3}(F+2G+2M)-1,\\ B&=\frac{1}{3}(F+2G-M),\\ C^2&=\frac{1}{3}\left[(F-G+M)^2-(F+2G-M)^2\right]. \end{aligned} \tag{A2}$$

Here F represents the interaction between Γ_{15}^v and Γ_1^c bands separated by the energy gap $\epsilon_0=\epsilon_g$ coupled with the matrix element P:

$$F=\frac{E_p}{\epsilon_0}=\frac{2P^2}{\epsilon_0}. \tag{A3}$$

M represents the interaction between Γ_{15}^v and Γ_{15}^c bands coupled by the matrix element Q

$$M=\frac{E_Q}{\epsilon_0^{*\prime}}=\frac{Q^2}{\epsilon_0'+2\Delta_0'/3}, \tag{A4}$$

with $\epsilon_0'^{*}=\epsilon_0'+2\Delta_0'/3$ being an effective ϵ_0' gap.

G represents the interaction between Γ_{15}^v and Γ_{12}^c bands and is relatively small in GaAs because of the large energy separation between these bands.

The values A, B, and C are connected with Luttinger parameters through the relations[15]

$$\gamma_1=A,\qquad \gamma_2=\frac{1}{2}B,\qquad \gamma_3=\frac{1}{6}(F-G+M). \tag{A5}$$

The signs in the above expressions are taken to make the parameters A, B, and the Luttinger parameters positive.

The equations above can be resolved with respect to parameters F, G, and M expressed in terms of Luttinger parameters γ_1, γ_2, and γ_3 as

$$M=\gamma_1-2\gamma_2+1, \tag{A6}$$

$$G=\frac{3}{2}(\gamma_1+\gamma_2-3\gamma_3+1), \tag{A7}$$

$$F=\gamma_1+4\gamma_2-2G. \tag{A8}$$

Term C in (A1) is responsible for the anisotropy of the valence band $C^2=12\left(\gamma_3^2-\gamma_2^2\right)$. In the case of small anisotropy $|\gamma_3-\gamma_2|\ll\gamma_2$ the following expressions can be derived for heavy- and light-hole cyclotron masses for $H\parallel(100)$:

$$m_{\rm hh}^{-1}=A-\sqrt{B^2+C^2/8}\approx\frac{3}{4}M+\frac{3}{8}G-1, \tag{A9}$$

$$m_{\rm lh}^{-1}=A+\sqrt{B^2+C^2/8}=\frac{2}{3}F+\frac{7}{12}M+\frac{23}{24}G-1 \tag{A10}$$

and for $H\parallel(111)$

$$m_{\rm hh}^{-1}=A-\sqrt{B^2+C^2/4}\approx\frac{1}{2}M+\frac{3}{4}G-1, \tag{A11}$$

$$m_{\rm lh}^{-1}=A+\sqrt{B^2+C^2/4}=\frac{2}{3}F+\frac{5}{6}M+\frac{7}{12}G-1. \tag{A12}$$

It follows from the symmetry of the bands involved and from Eqs. (A9)–(A12) that F does not couple the conduction band with the heavy-hole states and the heavy-hole mass is totally controlled by M and G.

The parameter F appears only in the expression for the light-hole mass and thus expression (A10) can be used to estimate F and check the consistency of P^2 with the value determined from conduction-band parameters. This estimate can be made by fixing the heavy-hole mass to its experimental value[9] and adjusting P to obtain agreement with the determined-light hole mass.

From $m_{\rm lh}=0.078m_0$, the matrix element P describing the coupling between Γ_1^c conduction and Γ_{15}^v valence band can be estimated ($E_P=2P^2=25$ eV). This value is much closer to estimates from conduction-band parameters [$E_P=26$ eV (Ref. 27) and $E_P=27.9$ eV (Ref. 23)] than that obtained from a previous set of valence-band parameters (the set of Luttinger parameters from Ref. 9 leads to $E_P=2P^2=22$ eV).

APPENDIX B: BAND NONPARABOLICITY

The solution of the Luttinger 4×4 Hamiltonian is linear in the magnetic field with the wave functions of $a^{\pm}$ and $b^{\pm}$ hole states dependent only on Landau quantum number and the direction but not the magnitude of H. A deviation from linear behavior on H occurs when higher-order terms in the expansion of $\varepsilon(k)$ are included. It is convenient to describe band nonparabolicity by an effective two band expression

$$\varepsilon=\varepsilon_1\left(1-\frac{\varepsilon_1}{\varepsilon^*}\right), \tag{B1}$$

where $\varepsilon_1 = \hbar^2 k^2/2m^*$ is the energy calculated in a parabolic band approximation, with m^* being the effective mass of the electron (hole) at the bottom of the band, and ε^* a parameter with the dimension of energy. This expression is connected with the conventional treatment of band nonparabolicity:[28]

$$\varepsilon(k) = \frac{\hbar^2 k^2}{2m^*} + \alpha_0 k^4 \tag{B2}$$

through the relation $\varepsilon^* = -\hbar^4/4(m^*)^2\alpha_0$.

Nonparabolic corrections to the cyclotron masses of electrons and holes have been considered in Refs. 19 and 16 within the framework of an 8×8 $\mathbf{k} \cdot \mathbf{p}$ matrix. For the quadratic corrections in H the following expressions were derived for conduction and light-hole bands:

$$\varepsilon_2^c = \left(1 - \frac{m_e^*}{m_0}\right)^2 (\varepsilon_1^c)^2 \left[\frac{3\varepsilon_0 + 4\Delta_0 + 2\Delta_0^2/\varepsilon_0}{(\varepsilon_0 + \Delta_0)(3\varepsilon_0 + 2\Delta_0)}\right], \tag{B3}$$

$$\varepsilon_2^{\rm lh} = \frac{\varepsilon_g + 2\Delta_0}{2\varepsilon_g \Delta_0} (\varepsilon_1^{\rm lh})^2, \tag{B4}$$

where ε_1^c and $\varepsilon_1^{\rm lh}$ are terms linear in H.

The expression for the conduction-band nonparabolicity was recently improved[29] in order to include coupling between Γ_1^c and Γ_{15}^c conduction bands represented by the matrix element P'. The following expression was obtained for the term $\alpha_0 k^4$:

$$\alpha_0 = -\frac{P^4}{E_0^{*3}} - \frac{P^2}{E_0^{*2}}\left(\frac{Q^2}{E_0'^*} - \frac{P'^2}{E_0'^* - E_0^*}\right) + \frac{P'^2 Q^2}{E_0^* \left(E_0'^* - E_0^*\right)^2}, \tag{B5}$$

where E_0^* and $E_0'^*$ are average gaps, $E_0^* = E_0 + \Delta_0/3 = 1.631$ eV, and $E_0'^* = E_0' + 2\Delta_0'/3 = 4.602$ eV. With parameters for GaAs taken from Ref. 27 we find from Eqs. (B4) and (B5) $\varepsilon_c^* = 1.31$ eV and $\varepsilon_{\rm lh}^* = 0.47$ eV.

The total nonparabolicity for the optical transitions can be written as

$$\varepsilon_2^{mn} = \frac{\left(\varepsilon_{1,n}^c\right)^2}{\varepsilon_c^*} + \frac{\left(\varepsilon_{1,m}^{\rm lh}\right)^2}{\varepsilon_{\rm lh}^*}. \tag{B6}$$

In the classical limit of large $n \gg 1$ (B6) can be written as

$$\varepsilon_2^{mn} = \left(n + \frac{1}{2}\right)^2 (\hbar\omega_c)^2 \times \left[1 + \left(\frac{m_e}{m_{\rm lh}}\right)^2 \frac{\varepsilon_c^*}{\varepsilon_{\rm lh}^*}\left(\frac{m + 1/2}{n + 1/2}\right)^2\right] \tag{B7}$$

with $m = n$ for $\Delta n = 0$ and $m = n + 2$ for $\Delta n = -2$ optical transitions. This approximate expression describes quite reasonably the observed dependence of experimentally measured nonparabolic coefficients $\epsilon_2(n)$ on the transition index n and also the difference in nonparabolicity between $b_n \rightarrow \beta_n$ and $a_{n+2} \rightarrow \alpha_n$ sets of transitions (see Fig. 9); the observed nonparabolicity, however, is 15–20 % stronger than that calculated with equations and parameters above.

APPENDIX C: COULOMB CORRECTIONS

The Coulomb interaction between electrons and holes decreases the energy of interband optical transitions and has to be taken into account. The calculations of the exciton binding energy are based on the adiabatic approximation which assumes that motion along the direction of magnetic field is slow compared with that in the xy plane perpendicular to the magnetic field. For the exciton ground state this requires that $\beta \gg 1$,[30] where 2β is the ratio of the cyclotron $\hbar\Omega = \hbar eH/\mu c$ to the Coulomb binding energy $R = \mu e^4/2\hbar^2\kappa_0$, i.e.,

$$\beta = \frac{\kappa_0 \hbar^3 H}{\mu^2 e^3 c}, \tag{C1}$$

where $\mu = m_e m_h/(m_e + m_h)$ is the exciton reduced mass and κ_0 the dielectric permittivity. Using for the relative motion a wave function of the form

$$\Psi(\rho, z) = (2\pi)^{-1/2} e^{iM\varphi} R(\rho, z) W(z), \tag{C2}$$

one can obtain after separation of variables two differential equations

$$\left[\frac{\hbar^2}{2\mu}\left(-\frac{1}{\rho}\frac{\partial}{\partial\rho}\rho\frac{\partial}{\partial\rho} + \frac{M^2}{\rho^2} + \frac{\rho^2}{4\lambda_H^2} + \frac{M}{\lambda_H^2}\right) - \frac{e^2}{\kappa_0 \left(\rho^2 + z^2\right)^{1/2}}\right] R(\rho, z) = V(z) R(\rho, z), \tag{C3}$$

$$\left(-\frac{\hbar^2}{2\mu}\frac{d^2}{dz^2} + V(z) - \varepsilon_\nu\right) W(z) = 0. \tag{C4}$$

Here $V(z)$ is a one-dimensional potential describing the relative motion of the electron and hole along the magnetic field direction, with ϵ_ν being the exciton binding energy, and $W(z)$ the wave function of this relative motion. $V(z)$ can be found from perturbation theory by using the Landau wave functions of free carriers as zeroth-order approximation. Perturbation theory gives satisfactory accuracy only for very high magnetic fields $\beta \gg 1$, while the adiabatic approximation itself is already valid for not very large $\beta \geq 1$.[31]

For excitons formed from higher Landau levels the binding energy depends on the magnetic field and Landau quantum number mainly through the effective Larmor radius of the exciton $L_R^{*2} = \lambda_H^2(n_\rho + |M| + 1)$.[21] Here the radial quantum number n_ρ is related to the Landau level number n and exciton magnetic number M through

$$n = n_\rho + \frac{|M| + M}{2}. \tag{C5}$$

This allows one to estimate the binding energy of an exci-

ton with a large quantum number n through the binding energy of the $n = 0$ state by means of the expression

$$\varepsilon_{ex}(n, \beta) = \varepsilon_{ex}(0, \beta^*) , \tag{C6}$$

where

$$\beta^* = \frac{H}{(n_\rho + |M| + 1)}. \tag{C7}$$

We have to note here that expression (C7) was deduced for parabolic bands. In semiconductors with degenerate bands one has to deal with a system of hole subbands which are characterized by different values of magnetic momentum and different longitudinal effective masses. The one-dimensional potential obtained from Eqs. (C3) and (C4) will be strongly dependent on the wave function admixture and will be different for $a^{\pm}$ and $b^{\pm}$ states even with the same Landau number.[31] To use expression (C7) in such a situation, we have to use different dependencies for the lower ($n = 0$) transition for $a^{\pm}, b^{\pm}$ hole ladders with corrections for the change of the longitudinal hole mass in each set. All this makes the procedure very complicated.

The situation simplifies drastically for the exciton states with large Landau indices $n \gg 1$. Gantmakher *et al.*[32] have shown that in this case the quasiclassical approach is valid, so that the problem can be solved analytically even for intermediate magnetic fields. They have also shown that the criterion for using the adiabatic approximation in this case is less strict, namely $\beta n > 1$.

The asymptotic potential $V(z)$ describing the one-dimensional motion was found to be in the quasiclassical approximation

$$V(z) = -\frac{2e^2}{\pi\kappa_0 (\rho_2^2 + z^2)^{1/2}} K\left[\left(\frac{\rho_2^2 - \rho_1^2}{\rho_2^2 - z^2}\right)^{1/2}\right] , \tag{C8}$$

where K is the elliptical integral of first kind and the turning points ρ_1 and ρ_2 are given by

$$\rho_{1,2}^2 = 4\lambda_H^2 \left\{2n - M + 1 \mp [(2n+1)(2n - M + 1)]^{1/2}\right\}. \tag{C9}$$

For $n \gg M$ the ground-state energy of an exciton with quantum numbers n and M was found to be[32]

$$\varepsilon = \hbar\Omega[n - (|M| + \gamma M)/2] + \frac{\hbar^2}{\mu a_B^* \rho_2 \pi}\left(\ln\frac{\pi a_B^*}{256\rho_2} + 1 - C\right) , \tag{C10}$$

where $a_B^* = \hbar^2\kappa/\mu^* e^2$ is the exciton radius, $\gamma = (m_e^* - m_h^*)/(m_e^* + m_h^*)$, and $C = 0.5772\ldots$ is the Euler constant.

Using for large n the longitudinal light-hole mass $m_{lh} = \gamma_1 + 2\gamma_2$ (Ref. 33), the estimate of Coulomb corrections to the energy of magneto-optical transitions can be made in a straightforward manner.

Coulomb corrections decrease rapidly with increasing Landau index n and with decreasing magnetic field. For large numbers $n \geq 4$ and magnetic fields in the range of 1 T< H <5 T these corrections give a contribution to the slope $\partial E/\partial H$ of less than 0.7 meV/T. This is small in comparison with the values $\partial E/\partial H \approx 15 - 35$ meV/T typical for transitions with $n = 4 - 10$. We note that neglecting exciton corrections during the fitting procedure gives for the light-hole mass even a lower value $m_{lh} = 0.075 m_0$.

*On leave from the Institute of Solid State Physics, Russian Academy of Sciences, 142432 Chernogolovka, Moscow District, Russia.

†Present address: Paul-Drude-Institut für Festkörperelektronik, D-1086, Berlin, Germany.

[1] Q. H. V. Vrehen, J. Phys. Chem. Solids **29**, 129 (1968).

[2] R. P. Seisyan, M. A. Abdulaev, and V. D. Drasnin, Fiz. Tekh. Poluprovodn. **7**, 807 (1973) [Sov. Phys. Semicond. **7**, 552 (1973)].

[3] K. Hess, D. Bimberg N. O. Lipari, U. Fishbach, and M. Altarelli, in *Proceedings of the 13th International Conference on the Physics of Semiconductors, Rome, 1976*, edited by F. G. Fumi (North-Holland, Amsterdam, 1976), p. 142.

[4] M. S. Skolnick, A. K. Jain, R. A. Stradling, J. Leotin, J. C. Ousset, and S. Askenazy, J. Phys. C **9**, 2809 (1976).

[5] C. Trallero-Giner, T. Ruf, and M. Cardona, Phys. Rev. B **41**, 3028 (1990); T. Ruf, R. T. Phillips, C. Trallero-Giner, and M. Cardona, *ibid.* **41**, 3039 (1990).

[6] B. V. Shanabrook, O. J. Glembocki, D. A. Broido, and W. I. Wang, Phys. Rev. B **39**, 3411 (1989).

[7] S. I. Gubarev, T. Ruf, M. Cardona, and K. Ploog, Solid State Commun. **85**, 853 (1993).

[8] R. P. Seisyan and M. A. Abdulaev, Fiz. Tekh. Poluprovodn. **7**, 811 (1973) [Sov. Phys. Semicond. **7**, 554 (1973)].

[9] *Physics of Group IV Elements and III-V Compounds*, edited by O. Madelung, M. Schmitz, and H. Weiss, Landolt-Börnstein Vol. 17a (Springer-Verlag, Berlin, 1982).

[10] W. Becker, B. Gerlach, T. Hornung, A. Nöthe, G. Spata, and R. G. Ulbrich, in *Proceedings of the 19th International Conference on the Physics of Semiconductors*, edited by W. Zawadzki (Polish Academy of Sciences, Warsaw, 1989), p. 1505.

[11] T. Ruf, R. T. Phillips, A. Cantarero, G. Ambrazevicius, M. Cardona, J. Schmitz, and U. Rössler, Phys. Rev. B **39**, 13 378 (1988).

[12] J. M. Luttinger and W.Kohn, Phys. Rev. **97**, 869 (1955).

[13] J. M. Luttinger, Phys. Rev. **102**, 1030 (1956).

[14] C. R. Pidgeon and R. N. Brown, Phys. Rev. **146**, 575 (1966).

[15] K. Suzuki and J. S. Hensel, Phys. Rev. B **9**, 4184 (1974).

[16] R. L. Aggarwal, in *Semiconductors and Semimetals*, edited by R. K. Willardson and A. C. Beer (Academic, New York, 1972), Vol. 9, 151.

[17] M. H. Weiler, R. L. Aggarwal, and B. Lax, Phys. Rev. B **17**, 3269 (1978).

[18] H.-R.Trebin, U. Rössler, and R. Ranvaud, Phys. Rev. B **20** 686 (1979).

[19] L. M. Roth, B. Lax, and S. Zwerdling, Phys. Rev. **114**, 90 (1959).

[20] M. H. Weiler, in *Semiconductors and Semimetals*, edited

by R. K. Willardson and A. C. Beer (Academic, New York, 1981) Vol. 16, p. 119.
[21]L. P. Nikitin, I. B. Rusanov, R. P. Seisyan, Al. L. Efros, and T. V. Yazeva, Fiz. Tekh. Poluprovodn. **16**, 1377 (1982) [Sov. Phys. Semicond. **16**, 883 (1982)].
[22]M. A. Hopkins, R. J. Nicholas, P. Pfeffer, W. Zawadzki, D. Gauthier, J. C. Portal, and M. A. DiForte-Poisson, Semicond. Sci. Technol. **2**, 568 (1987); H. Sigg, J. A. Perenboom, P. Pfeffer, and W. Zawadzki, Solid State Commun. **61**, 685 (1987).
[23]P. Pfeffer and W. Zawadzki, Phys. Rev. B **41**, 1561 (1990).
[24]C. Trallero-Giner, F. Iikawa, and M. Cardona, Phys. Rev. B **44**, 12815 (1991).
[25]F. M. Peters and J. T. Devreese, Phys. Rev. B **31**, 3589 (1985).
[26]G. Dresselhaus, A. F. Kip, and C. Kittel, Phys. Rev. **98**, 368 (1955).
[27]M. Cardona, N. E. Christensen, and G. Fasol, Phys. Rev. B **38**, 1806 (1988).
[28]U. Rössler, Solid State Commun. **49**, 943 (1984).
[29]T. Ruf and M. Cardona, Phys. Rev. B **41**, 10747 (1990).
[30]R. J. Elliot and R. Loudon, J. Phys. Chem. Solids **8**, 382 (1959); **15**, 196 (1960).
[31]B. L. Gelmont, R. P. Seisyan, Al. L. Efros, and A. V. Varfolomeev, Fiz. Tekh. Poluprovodn. **11**, 238 (1977) [Sov. Phys. Semicond. **11**, 139 (1977)].
[32]V. F. Gantmakher, B. L. Gel'mont, V. N. Zverev, and Al. L. Efros, Zh. Eksp. Teor. Fiz. **84**, 1129 (1982) [Sov. Phys. JETP **57**, 656 (1982)].
[33]C. Hermann and C. Weisbuch, Phys. Rev. B **15**, 823 (1977).